Available online at www.sciencedirect.com
ScienceDirect
Optics Communications 273 (2007) 538–543
OPTICS COMMUNICATIONS
www.elsevier.com/locate/optcom

Optical nonlinearities of Au nanoparticles embedded in a zinc oxide matrix

A.I. Ryasnyanskiy [a,*], B. Palpant [a], S. Debrus [a], U. Pal [b], A.L. Stepanov [c]

[a] Institut des Nano-Sciences de Paris, Université Pierre et Marie Curie – Paris 6, Université Denis Diderot – Paris 7, CNRS, UMR 7588, 140 rue de Lourmel, 75015 Paris, France
[b] Instituto de Física, Universidad Autónoma de Puebla, Apdo. Postal J-48, Puebla, Pue. 72570, Mexico
[c] Kazan Physics-Technical Institute, Russian Academy of Sciences, 420029 Kazan, Russian Federation

Received 11 September 2006; received in revised form 7 November 2006; accepted 11 January 2007

Abstract

Optical nonlinearities of Au nanoparticles embedded in zinc oxide (ZnO) matrix have been investigated by the *Z*-scan method at the wavelength of 532 nm using nanosecond Nd^{3+}:YAG laser radiation. The nonlinear refractive index has been measured and the real part of the third-order nonlinear susceptibility is deduced. The results of the investigation of nonlinear refraction using the off-axis *Z*-scan configuration are presented and the mechanisms responsible for the nonlinear response are discussed. The nonlinear refraction is found to be negative (self-defocusing) in the vicinity of the surface plasmon resonance. Moreover, its strength is shown to be larger for materials having higher gold concentration. Finally, the prevailing influence of the electronic Kerr effect over the possible thermo-optical contribution is demonstrated.

Keywords: Gold nanoparticles; ZnO; Nonlinear refraction; *Z*-scan

1. Introduction

The optical Kerr effect corresponds to a third-order nonlinear optical process where the refractive index of a medium, n, varies linearly with the incident intensity I as: $n = n_0 + \gamma I$, where n_0 is the linear refractive index and γ is the nonlinear refraction coefficient. The sign and value of γ for a particular material are very much important for its practical applications. The γ value can be positive when the medium behaves like a focusing lens, and negative in the case where it diverges laser radiation. Knowledge of these parameters is important when choosing the application area of a material. For example, a material with positive sign of γ can be used for soliton formation in optical waveguides [1,2] and a material characterized by a negative sign of γ and a low efficiency of nonlinear absorption can be applied as an optical limiter of laser radiation [3,4] due to the divergence produced by self-defocusing. To understand and further improve such properties, the important point is to determine the origin of the nonlinear refraction mechanism, which can influence both the value and sign of γ.

Metal nanoparticle systems like metal-doped glasses or colloidal solutions are of considerable interest due to fast response time on laser excitation [5,6] and large value of the third-order nonlinear susceptibility, $\chi^{(3)}$, responsible for Kerr effect [7–10]. Optical nonlinearities of gold nanoparticles were the subject of numbers of investigations during the past decade. The influences of nanoparticle parameters (size and shape), preparation methods (ion implantation, r.f. sputtering, chemical, sol–gel, etc.) together with laser radiation parameters (pulse duration, repetition rate, wavelength, etc.) on the nonlinear optical properties of materials were considered. The characteristics of the surrounding matrix were also the subject of

* Corresponding author.
E-mail address: ryasn2000@yahoo.com (A.I. Ryasnyanskiy).

0030-4018/$ - see front matter © 2007 Elsevier B.V. All rights reserved.
doi:10.1016/j.optcom.2007.01.013

numerous investigations. Thus, for example, water [11–14], silicate glass [1,7–9], $BaTiO_3$ [15], Al_2O_3 [16,17], $LiNbO_3$ [18], TiO_2 [19] were applied for composite material optimization to obtain appropriate values of the nonlinear optical coefficients. As example, in Table 1, some published results regarding the third-order nonlinear susceptibilities of various composite materials with gold nanoparticles in the visible range are collected.

One of the interesting points now is the search for a new matrix for the creation of composite materials with high values of nonlinear optical parameters. Recently we showed the possibility of fabricating a new material, Cu:ZnO [20], with high value of the nonlinear absorption coefficient [21,22], which can be used for optical limiting in the visible spectral range and as an element for reducing laser intensity fluctuations.

Among the experimental methods used for the investigation of nonlinear properties of materials, the most comfortable and informative is the *Z*-scan technique [23] which allows the determination of both the value and sign of γ when other methods, for example, degenerate four-wave mixing, give information about the absolute value of γ only. In the present paper the *Z*-scan technique was used for determining the value and sign of the nonlinear refraction coefficient and the real part of the third-order nonlinear susceptibility of composite materials consisting of Au nanoparticles in ZnO.

2. Experimental

2.1. Sample preparation and structure characterization

Au–ZnO composite thin films were prepared on flat quartz substrates (Nihon Rika Garasu Kogio) using a radio-frequency (r.f.) co-sputtering technique. During sputtering process three pieces of Au wires with a diameter of 0.4 mm of either 1 mm (sample 1) or 3 mm lengths (sample 2) were placed on a 100 mm diameter ZnO target (10 cm diameter, 99.99% purity) and sputtered simultaneously at 100 W power in the chamber with 10^{-2} Torr argon pressure for 1 h. Thus, two samples with different quantities of deposited gold were fabricated (Table 2). The thicknesses of the composite film samples 1 and 2, measured by a Dektak II profilometer were of 855 and 930 nm respectively. After deposition they were annealed at 320 °C for 2 h in argon atmosphere.

For transmission electron microscopy (TEM) observations, the composite films about 25 nm thick were deposited on carbon-coated NaCl substrates and transferred subsequently to the microscopic copper grids by floating on water surface. A JEOL JEM2000-FXII electron microscope was used for observing the samples. The composition of the fabricated films was evaluated through a Perkin–Elmer (PHI 5600ci) X-ray photoelectron spectroscopy (XPS) system. A Shimadzu UV–VIS 3101PC double-beam spectrophotometer was used to record the linear optical absorption spectra of the samples. Details regarding sample preparation and properties can be found in [29,30].

2.2. Optical nonlinearity measurements

Among the methods developed for investigating the nonlinear optical parameters of materials, the *Z*-scan one [23] has some advantages over others due to the possibility of complete measurements of the nonlinear refraction coefficient γ. The *Z*-scan scheme with closed aperture [23] was used in our experiment for the investigation of nonlinear refraction in the nanocomposite samples. A frequency-doubled Q-switched Nd^{3+}:YAG laser (pulse duration: $\tau = 7$ ns, wavelength: $\lambda = 532$ nm, repetition rate: 10 Hz) was used. The working wavelength is very close to the spectral location of the SPR maximum in the samples (see Section 3). The detailed description of our conventional experimental set-up is given in [31]. An extra improvement of the equip-

Table 1
Nonlinear optical properties of Au nanoparticles in different matrices

Matrix	λ_{SPR} (nm)	Laser parameters	Investigation method	$\mathrm{Re}[\chi^{(3)}]$ (esu)	$\lvert\chi^{(3)}\rvert$ (esu)	References
Water	525	$\tau = 35$ ns, $\lambda = 527$ nm	*Z*-scan	-4.5×10^{-11}	–	[24]
$BaTiO_3$	690	$\tau = 120$ fs, $\lambda = 800$ nm	OKE	–	1.3×10^{-10}	[25]
ZrO	574	$\tau = 120$ fs, $\lambda = 800$ nm	OKE	–	$\sim3.3\times10^{-10}$	[25]
Silicate glass	~550	$\tau = 70$ ps, $\lambda = 532$ nm	DFWM	–	2.5×10^{-6}	[26]
TiO_2	647	$\tau = 250$ fs, $\lambda = 750$ nm	*Z*-scan	-1.11×10^{-7}	1.1×10^{-7}	[27]
TiO_2	680	$\tau = 200$ fs, $\lambda = \sim680$ nm	DFWM	–	6.0×10^{-7}	[19]
Al_2O_3	625	$\tau = 7$ ns, $\lambda = 532$ nm	*Z*-scan	-1.55×10^{-5}	–	[28]

λ_{SPR} is the wavelength of surface plasmon resonance maximum, τ is the laser pulse-width, and λ is the laser wavelength.
OKE – Optical Kerr effect measurement technique, DFWM – Degenerate four-wave mixing.

Table 2
Nonlinear optical parameters of Au–ZnO composites

Sample	SPR maximum (nm)	Au atom concentration (atom %)	I_{00} (MW cm^{-2})	γ (10^{-10} cm^2 W^{-1})	$\mathrm{Re}[\chi^{(3)}]$ (10^{-8} esu)
1	–	7.82	9.3	−6.78	−7.58
2	540	8.68	7.9	−13.1	−14.7

ment consists in adding a second reference arm having exactly the same optical path as the closed-aperture detection arm, except from the sample, in order to reduce the detection noise stemming from pulse-to-pulse beam pointing fluctuations, as proposed in [21]. So, the energy of radiation transmitted through the sample and aperture was normalized to the energy of incident radiation transmitted just through the aperture.

The experimental optical conditions were as follows: beam waist = 50 μm, distance from the focus to the aperture = 90 cm, confocal beam parameter = 1.48 cm, aperture radius = 1 mm.

The off-axis Z-scan experiments took place at the same conditions as for conventional Z-scan scheme except that the transverse position of the aperture with respect to the axis of the beam was changed. The distance from the beam axis to the aperture center was varied from 4 to 5 mm. To investigate the temporal characteristics of radiation, fast photodiode detectors with a response time of ~500 ps were used. The intensity of the laser beam in the lens focus (I_{00}) was in the range of 6×10^6 to 1×10^7 W cm^{-2}, which is below the optical breakdown threshold of the present samples. The experiments were carried out at different radiation intensities for several times at the same point on the sample to be sure that there were no structural changes in materials, what was confirmed from a good reproducibility of the obtained results.

3. Results

3.1. TEM and linear optical absorption spectroscopy

Fig. 1 shows the TEM micrographs of the samples 1 and 2, prepared with low (Fig. 1a) and high (Fig. 1b) concentration of Au, respectively. As it can be seen from the figure, roughly spherical gold nanoparticles are created in the ZnO matrix by r.f. co-sputtering. XPS results reveal the incorporation of about 7.8 and 8.7 at.% of Au in the composite films 1 and 2, respectively. Size of gold nanoparticles varied from 1 to 30 nm with the maximum at 7.5 nm for sample 1 and from 2 to 28 nm with the maximum at 15 nm for sample 2.

The linear optical absorption spectra of the samples investigated are shown in Fig. 2. It can be observed that samples 1 and 2 exhibit an increased selective absorption in the region near 540 nm, superimposed on the monotonous

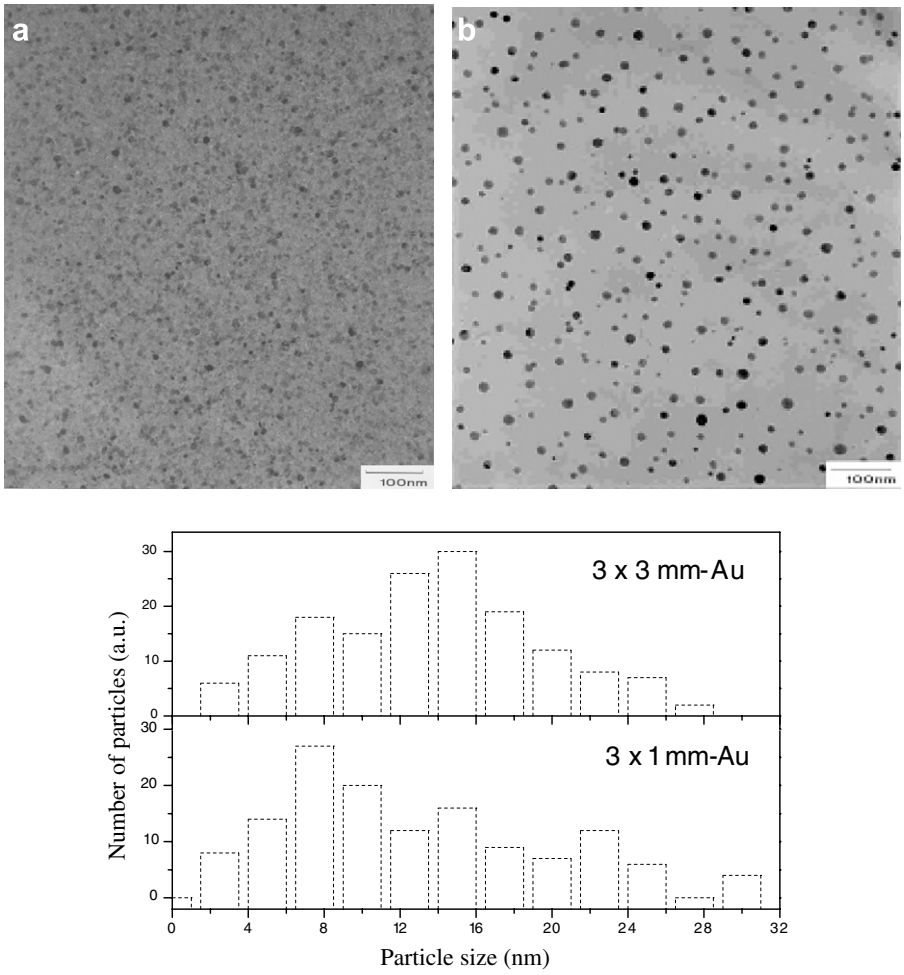

Fig. 1. TEM micrographs of Au–ZnO nanocomposite films (a) sample 1, and (b) sample 2, along with their size distribution histograms (bottom).

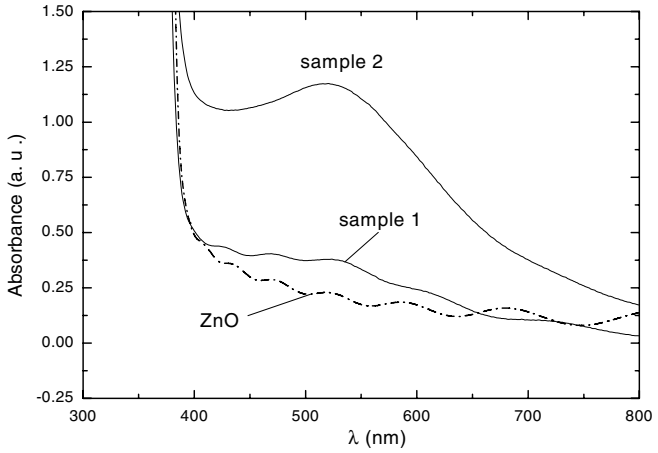

Fig. 2. Linear optical absorption spectra of the Au–ZnO samples 1 and 2. The absorption spectrum of ZnO film (840 nm thick) without Au is also presented as reference.

absorption stemming from interband transitions in gold nanoparticles. This selective absorption band is due to the surface plasmon resonance (SPR) that is extra evidence of Au nanoparticle formation. However, the intensity of this SPR absorption is obviously higher in sample 2 than in sample 1. The weak spectral oscillations observed on sample 1 spectrum between 400 and 800 nm originate from light interferences in the thin films. They are not present in sample 2 due to its high absorption. All these elements indicate that, even if the metal concentrations are close from one sample to another, a large part of gold is present in sample 1 as atoms or very small particles, whereas it is packed into larger nanoparticles in sample 2. This is confirmed by the examination of TEM micrographs (Fig. 1), despite the fact that very small particles cannot be distinguished from the gray background. Due to higher content of Au in sample 2, the aggregation process on thermal annealing is prominent.

3.2. Nonlinear optical measurements

The results of the measurements of γ for both samples are presented in Fig 3. As can be seen, the profiles show a maximum of normalized transmittance $T(z)$ before focus with further minimum after focus, which characterizes a negative refractive index: both samples exhibit self-defocusing properties [23].

By defining the relative coordinate $x = z/z_0$, z_0 being the diffraction length, the spatial dependence of the normalized transmission T in the case of nonlinear refraction can be written as proposed in [23]

$$T(x) = 1 - \frac{4x}{(x^2+9)(x^2+1)}\Delta\Phi_0. \quad (1)$$

$z_0 = 0.5kw_0^2$, $\Delta\Phi_0 = k\gamma I_{00}L_{\text{eff}}$, $k = 2\pi/\lambda$ is the wave number, w_0 is the beam waist radius at focus, $L_{\text{eff}} = [1 - \exp(-\alpha_0 L)]/\alpha_0$ is the effective sample length, L is the real sample length (in our case L is the thickness of the layer with gold nanoparticles) and α_0 is the linear absorption coefficient, which has been calculated from the absorption spectra of the samples.

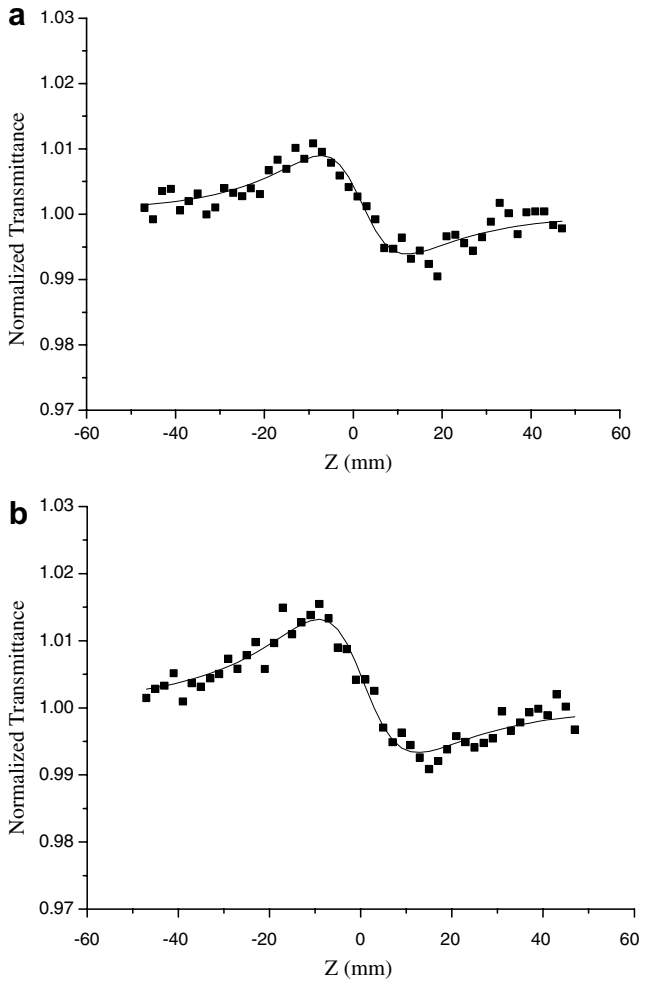

Fig. 3. Z-scan profile of the normalized transmittance measured for (a) sample 1 and (b) sample 2 in the closed aperture Z-scan scheme. Solid lines are the best theoretical fits (Eq. (1)).

Using Eq. (1) the theoretical curves were fitted to experimental data and the values of γ and $\text{Re}[\chi^{(3)}]$ were determined (see Table 2) using the following expression [23]:

$$\gamma = \frac{120\pi^2}{n_0^2 c}\text{Re}[\chi^{(3)}], \quad (2)$$

where c denotes the light velocity in vacuum. In Eq. (2), γ is expressed in $\text{cm}^2\,\text{W}^{-1}$ and $\text{Re}[\chi^{(3)}]$ in electrostatic units (esu). One can see from the table that the value of γ and $\text{Re}[\chi^{(3)}]$ is higher for the sample with higher gold concentration. Such a feature was previously observed as reported in numerous publications, in particular for gold in silica [10,26] or TiO_2 [19].

In order to prove the validity of the conventional measurements of the sign of nonlinear refractive index presented in Fig 4 we used the Z-scan technique in the off-axis configuration [4,32,33]. This technique allows enhancing the sensitivity of the measurement of γ by analyzing the phase change at the edge of the beam rather than at the

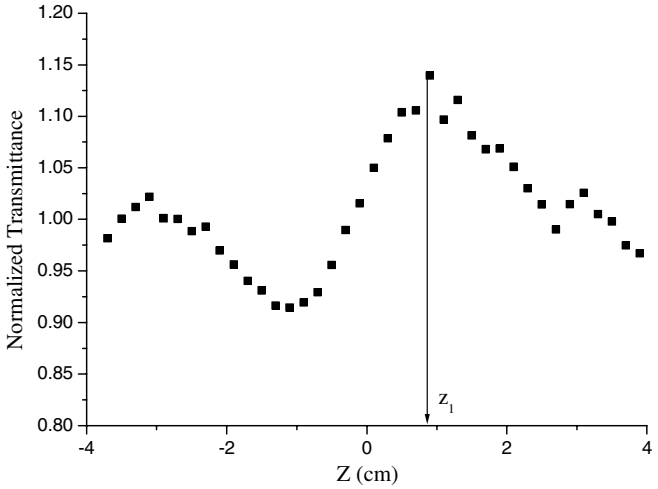

Fig. 4. Normalized transmittance dependence for sample 1 measured in the closed aperture off-axis Z-scan scheme. The arrow and position z_1 denote the transmittance maximum location.

beam center like in conventional Z-scan [23]. Thus, in Fig. 4 the $T(z)$ profile is shown for sample 2 in the off-axis Z-scan configuration One can see from the illustration the change of the priority of transmission maximum and minimum. $T(z)$ maximum for off-axis Z-scan is observed for positive z values while for conventional Z-scan measurements (Fig 3b) it is in the region of negative z values. This fact confirms the conventional method result. Indeed, for off-axis Z-scan the normalized transmittance is measured in the aperture plane at the beam edge instead of the center. Diverging light will increase the transmittance for the beam edge and decrease it at the center. On the contrary, converging light will decrease transmittance at the beam edge and increase it at the center.

4. Discussion

The sputtered gold in the composite films forms well dispersed nanoparticles in the ZnO matrix. The mean size of the Au particles increases with the gold content in the films.

First, it should be noted that the value of the nonlinear refractive index for ZnO ($\gamma = -0.9 \times 10^{-14}$ cm^2 W^{-1} [34]) is much smaller than the determined experimentally here (see Table 2). So, it shows that optical nonlinearities of the composite materials investigated originate from gold nanoparticles.

We now consider possible mechanisms for nonlinear refraction in our samples. A large contribution to the measured value of the nonlinear refractive index of composite materials can stem from a thermal lens effect, especially for laser pulses with long duration. This effect can be considered as a result of significant energy transfer from heated metal nanoparticles to the surrounding dielectric during the pulse passage [24,35]. The time which is necessary for this process to settle, τ_{tl}, can be roughly estimated as the ratio of the laser beam radius at focus, w_0, to the sound velocity in the dielectric matrix, v_s. Taking into account experimental conditions ($w_0 = 35$ μm, $v_s = 6590$ m s^{-1} for ZnO [36]) the value of τ_{tl} is calculated to be 5.3 ns. It means that such a thermal lens effect may occur significantly at the end of the pulse passage in the material, since the pulse duration is 7 ns. It should also be noted that a cumulative thermal effect can develop if pulsed lasers with high repetition rate are used (kHz or MHz [37]). However, in our experiments laser radiation with low repetition rate (10 Hz) has been used, thus preventing a cumulative thermal effect.

To be sure that the electronic effect in Au nanoparticles is the main mechanism of nonlinear refraction in composite samples we have performed the measurements of temporal characteristics of the radiation transmitted through the sample and aperture in the off-axis configuration. For this purpose we moved the aperture to 4.5 mm from the axis of laser beam. This method was applied earlier in experiments with colloidal gold [24], where a temporal and amplitude shift of the transmitted pulses was observed. The experimental conditions were the same as the ones used for the results of Fig. 4. The sample was kept at the region of maximum transmission (see Fig. 4, position z_1). The corresponding oscilloscope traces are presented in Fig 5. One can see that the only noticeable change concerns the amplitude of the transmitted pulse. There is no temporal shift for the transmitted pulse, which can be the proof of negligible influence of thermal effect in comparison with electronic one in our experiments. It should be noted that such measurements were performed for sample 2 also with the same result.

The third-order nonlinear response of the present composite materials thus mainly originates from pure electronic effects in gold nanoparticles. These electronic contributions are due to both intraband and interband transitions. The first one corresponds to transitions within the conduction band and the second one to transitions from the upper levels of the filled d band to the levels above the Fermi level in the conduction band. Whereas the only intraband contribution to the nanoparticle intrinsic third-order susceptibility is thought to be size-dependent, it is dominated by the

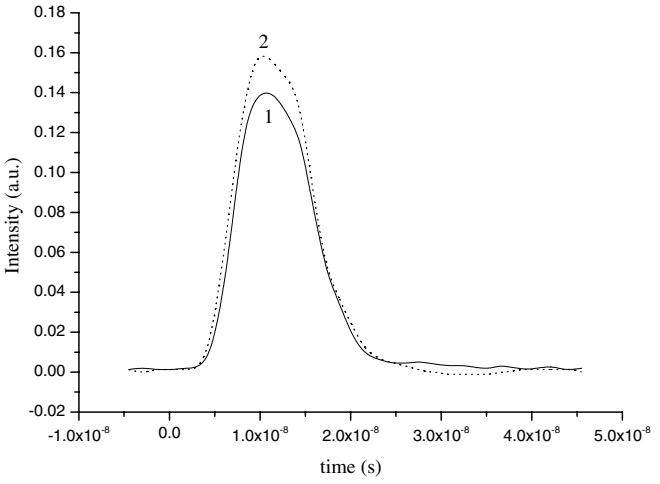

Fig. 5. Temporal pulse profiles for sample 1. Solid line (1): reference beam. Dotted line (2): beam transmitted through the sample and aperture.

size-independent interband contribution in the SPR spectral domain [38,39]. In the case where the particles are excited by ultra-short laser pulses a hot electron phenomenon (also called Fermi smearing) may superimpose on the pure electronic nonlinear contributions to $\chi^{(3)}$ [38]. When using nanosecond pulse-width excitation as in the present experiments, however, such a contribution is negligible [35,40].

5. Conclusion

The Z-scan method was applied in this work for the analysis of the nonlinear refractive optical properties of nanocomposite materials consisting of gold nanoparticles embedded in a zinc oxide matrix. The nonlinear refraction coefficient and the real part of the third-order nonlinear susceptibility were determined in the close vicinity of the SPR maximum using nanosecond radiation produced by a frequency-doubled Nd^{3+}:YAG laser. The value of γ was measured to be -6.78×10^{-10} cm^2 W^{-1} and -13.1×10^{-10} cm^2 W^{-1} for samples 1 and 2, respectively. The corresponding value of $\mathrm{Re}[\chi^{(3)}]$ is worth -7.58×10^{-8} esu and -14.7×10^{-8} esu. It was shown that the absolute values of γ and $\mathrm{Re}[\chi^{(3)}]$ are larger for materials having higher gold concentration, below the percolation threshold. On the basis of investigation of the temporal characteristic of radiation transmitted through the samples it was possible to deduce the prevailing influence of electronic Kerr effect in the nonlinear response.

Acknowledgements

A.I.R. acknowledges the financial support of the INTAS foundation (Grant No. 05-109-4749). A.L.S. is grateful to the Alexander Humboldt Foundation (Germany) and the Austrian Scientific Foundation in the frame of Lise Meitner program for the financial support. This study was sponsored partly by the Federal Program for Support of the Leading Scientific Schools of Russian Federation (Grant No. NSh 1904.2003.2), the Russian Foundation for basic Research (Grant No. 04-02-97505 and Grant No. 06-02-08147-ofi), the OFN of Russian Academy of Sciences "Advanced Materials and Structures" and also CONACyT (Grant No. 46269), Mexico.

References

[1] Y.S. Kivshar, W. Królikowski, O.A. Chubukalo, Phys. Rev. E 50 (1994) 5020.
[2] H.S. Eisenberg, Y. Silberberg, R. Morandotti, A.R. Boyd, J.S. Aitchison, Phys. Rev. Lett. 81 (1998) 3383.
[3] B.L. Justus, A.L. Huston, A.J. Campillo, Appl. Phys. Lett. 63 (1993) 1483.
[4] B.L. Justus, Z.H. Kafafi, A.L. Huston, Opt. Lett. 18 (1993) 1603.
[5] O.P. Varnavski, T. Goodson, M.B. Mohamed, M.A. El-Sayed, Phys. Rev. B 72 (2005) 235405.
[6] H. Inouye, K. Tanaka, I. Tanahashi, Y. Kondo, K. Hirao, J. Phys. Soc. Jpn. 68 (1999) 3810.
[7] R.A. Ganeev, A.I. Ryasnyanskiy, A.L. Stepanov, T. Usmanov, Phys. Stat. Sol. B 241 (2004) R1.
[8] R.A. Ganeev, A.I. Ryasnyanskiy, A.L. Stepanov, T. Usmanov, Phys. Status Solidi B 4 (2004) 935.
[9] R.A. Ganeev, A.I. Ryasnyanskiy, A.L. Stepanov, T. Usmanov, Opt. Quant. Electron. 36 (2004) 946.
[10] N. Pinçon, B. Palpant, D. Prot, E. Charron, S. Debrus, Eur. Phys. J. D 19 (2002) 395.
[11] R.A. Ganeev, M. Baba, A.I. Ryasnyasnkiy, M. Suzuki, H. Kuroda, Opt. Commun. 240 (2004) 437.
[12] L. Francois, M. Mostafavi, J. Belloni, J.F. Delouis, J. Delaire, P. Feneyrou, J. Phys. Chem. B 104 (2000) 6133.
[13] R.A. Ganeev, A.I. Ryasnyanskiy, Sh. R. Kamalov, N.V. Kamanina, I.A. Kulagin, M.K. Kodirov, T. Usmanov, Nonlin. Opt. 28 (2002) 263.
[14] R.A. Ganeev, A.I. Ryasnyanskiy, S.R. Kamalov, M.K. Kodirov, T. Usmanov, J. Phys. D: Appl. Phys. 34 (2001) 1602.
[15] G. Yang, W.-T. Wang, G.-Z. Yang, Z.-H. Chen, Chinese Phys. Lett. 20 (2003) 924.
[16] J.M. Ballesteros, R. Serna, J. Solis, C.N. Afonso, A.K. Petford-Long, D.H. Osborne, R.F. Haglund Jr., Appl. Phys. Lett. 71 (1997) 2445.
[17] R.A. Ganeev, A.I. Ryasnyanskiy, A.L. Stepanov, C. Marques, R.C. da Silva, E. Alves, Opt. Commun. 253 (2005) 205.
[18] S.S. Sarkisov, E. Williams, M. Curley, D. Ila, P. Venkateswarlu, D.B. Poker, D.K. Hensley, Nucl. Inst. Meth. Phys. Res. 141 (1998) 294.
[19] H.B. Liao, R.F. Xiao, J.S. Fu, H. Wang, K.S. Wong, G.K.L. Wong, Opt. Lett. 23 (1998) 388.
[20] A.L. Stepanov, R.I. Khaibullin, N. Can, R.A. Ganeev, A.I. Ryasnyanskiy, C. Buchal, S. Uysal, Tech. Phys. Lett. 30 (2004) 8.
[21] A.I. Ryasnyanskiy, B. Palpant, S. Debrus, R.A. Ganeev, A.L. Stepanov, N. Can, C. Buchal, S. Uysal, Appl. Opt. 44 (2005) 2839.
[22] T. Karali, N. Can, L. Valberg, A.L. Stepanov, P.D. Townsend, C. Buchal, R.A. Ganeev, A.I. Ryasnyanskiy, H.G. Belik, M.L. Jessett, C. Ong, Physica B 363 (2005) 88.
[23] M. Sheik-Bahae, A.A. Said, T.-H. Wei, D.J. Hagan, E.W. Van Stryland, IEEE J. Quant. Electron. 26 (1990) 760.
[24] C.S. Mehendale, S.R. Mishra, K.S. Bindra, M. Laghate, T.S. Dhami, K.S. Rustagi, Opt. Commun. 133 (1997) 273.
[25] G. Ma, W. Sun, S.-H. Tang, H. Zhang, Z. Shen, Opt. Lett. 27 (2002) 1043.
[26] H.B. Liao, R.F. Xiao, J.S. Fu, G.K.L. Wong, Appl. Phys. B 65 (1997) 673.
[27] M. Kyoung, M. Lee, Bull. Korean Chem. Soc. 21 (2000) 26.
[28] A.I. Ryasnyanskiy, B. Palpant, S. Debrus, Phys. Rev. B, submitted for publication.
[29] U. Pal, E. Aguila Almanza, O. Vázquez Cuchillo, N. Koshizaki, T. Sasaki, S. Terauchi, Sol. Energ. Mater. Sol. Cells 70 (2001) 363.
[30] U. Pal, J. García-Serrano, G. Casarrubias-Segura, N. Koshizaki, T. Sasaki, S. Terahuchi, Sol. Energ. Mat. Sol. Cells 81 (2004) 339.
[31] S. Debrus, J. Lafait, M. May, N. Pinçon, D. Prot, C. Sella, J. Venturini, J. Appl. Phys. 88 (2000) 4469.
[32] J.-G. Tian, W.-P. Zang, G. Zhang, Opt. Commun. 107 (1994) 415.
[33] A.I. Ryasnyanskiy, B. Palpant, Appl. Opt. 45 (2006) 2.
[34] X.J. Zhang, W. Ji, S.H. Tang, J. Opt. Soc. Am. B 14 (1997) 1951.
[35] M. Rashidi-Huyeh, B. Palpant, J. Appl. Phys. 96 (2004) 4475.
[36] D.C. Look, Sem. Sci. Tech. 20 (2005) S55.
[37] M. Falconieri, G. Salvetti, E. Cattaruza, F. Gonella, G. Mattei, P. Mazzoldi, M. Piovesan, G. Battaglin, R. Polloni, Appl. Phys. Lett. 73 (1998) 288.
[38] F. Hache, D. Ricard, C. Flytzanis, U. Kreibig, Appl. Phys. A 47 (1988) 347.
[39] M.J. Bloemer, J.W. Haus, P.R. Ashley, J. Opt. Soc. Am. B 7 (1990) 790.
[40] B. Palpant, D. Prot, A.-S. Mouketou-Missono, M. Rashidi-Huyeh, C. Sella, S. Debrus, Proc. SPIE 5221 (2003) 14.